Journal of Mathematical Modeling
Vol. 8, No. 2, 2020, pp. 123-138

JMM

Numerical simulation of the biosensors in a trigger mode based on Michaelis-Menten enzymatic reaction

Maryam Abjadian[†], **Ameneh Taleei**[†*]

[†]*Department of Mathematics, Shiraz University of Technology, Shiraz, Iran*

Email(s): baharabjadian@gmail.com, a.taleei@sutech.ac.ir

Abstract. An amperometric biosensor in trigger mode is a type of biosensor which is used to improve the sensitivity and specificity of the detection event by coupling different enzymes. In this paper, we study a numerical scheme to solve the one-dimensional diffusion-reaction equations with a nonlinear term related to Michaelis-Menten kinetics of the enzymatic reactions. In order to simulate numerically the model under study, we discretize the time variable with a semi-implicit backward Euler approach. Also, we use the meshfree collocation method based on thin plate spline radial basis function for the discretization of the spatial derivative. The biosensor response with and without amplification has been compared. The influence of the normalized Michaelis constant, the maximal enzymatic rate and substrate concentration on the triggering biosensor response is investigated.

Keywords: Biosensor, trigger mode, Michaelis-Menten kinetics, thin plate spline radial basis function.
AMS Subject Classification 2010: 35K57, 65N06, 65N35.

1 Introduction

A biosensor is an analytical device that contains a biological material such as tissues, micro-organism and cell receptors [17]. The enzyme in the

*Corresponding author.
Received: 19 August 2019 / Revised: 12 February 2020 / Accepted: 17 February 2020.
DOI: 10.22124/jmm.2020.14147.1307

biosensor discerns the substrate to be measured and specifically converts it into a product of the biochemical reaction [21]. Amperometric biosensor is a type of biosensor which converts a biochemical reaction process into a measurable signal using transducer [2]. These low-cost biosensors are used in biotechnology, medicine and environmental monitoring [12]. However, amperometric biosensor possess a number of serious drawbacks. One of the most important drawbacks is the short linear range of the calibration curve that restricts wider use of the biosensors [6]. In terms of increasing the range of analytes that may be detected, and the sensitivity and specificity of the detection event have to couple diffrent enzymes. Chemical amplification is known as a powerful approach for increasing the sensitivity of biosensors [8,9,24]. We can achieve this by cyclic conversion of substrates. If a biosensor contains an enzyme that starts analyte conversion following the cyclic product conversion the scheme of the biosensor action can be called as "triggering". In this paper, we study the numerical simulation of two mathematical models of biosensors acting, CCE and CEC schemes, in a trigger mode. While the CCE scheme is applied as a framework to investigate the behaviour of biosensors utilizing a trigger enzymatic reaction following enzymatic and electrochemical conversion of the product, the other model (CEC scheme) expresses the behaviour of biosensors utilizing a trigger enzymatic reaction following the electrochemical and enzymatic product cyclic conversion [1, 2, 16].

As far as we know, there are not too much work relating to the numerical simulation of the models under study. Baronas et al. studied the finite difference method for these biosensors [1,2].The main aim of this paper is to show that the meshfree collocation method based on thin plate spline (TPS) radial basis function (RBF) is also suitable for the numerical simulation of the biosensors in a trigger mode. The RBFs method is known as a powerfull tool for scattered data interpolation and is used actively for solving partial differential equations [4, 10, 11, 15, 18, 19]. Since the numerical modeling of biosensors with complex geometry such as biosensor based on heterogeneous microreactor, plate-gap biosensor and biosensor with selectived and perforated membranes are very important problems [3,13,14,20,22,23], this study can be useful for further research on the models under investigation.

The layout of the article is as follows: In Section 2, we provide a brief review of the radial basis function collocation method based on TPS radial basis function. In Section 3, we describe two mathematical models of biosensors acting in a trigger mode. In this section, we also discretize the obtained non-linear diffusion-reaction equations by using the semi-implicit backward Euler approch in time and the radial basis function collocation

method based on TPS in space. The numerical simulation for both schemes, CEC and CCE, are investigated in Section 4. Finally, the conclusion is presented in Section 5.

2 The radial basis function collocation method

Let $\mathbf{x}^* \in \mathbb{R}^d (d = 1, 2, 3)$. The radial basis function $\phi : \mathbb{R}^d \longrightarrow \mathbb{R}$ is an invariant function whose value at any point $\mathbf{x} \in \mathbb{R}^d$ depends only on the distance from the fixed point $\mathbf{x}^*$. This function can be written $\phi(r) = \phi(\|\mathbf{x} - \mathbf{x}^*\|)$ where $\|.\|$ is the Euclidian norm and $\mathbf{x}^*$ is the center of RBF ϕ. Some classical choices of ϕ, such as multiquadrics, inverse multiquadrics and Gaussian basis functions are dependent on a free shape parameter. This shape parameter has an important role in the approximation of the RBF method. In this study, we use TPS radial basis function since it does not require a free shape parameter and its solution is not dependent on the shape parameter [5]. More details on RBFs can be found in [7]. The TPS function can be defined as $\phi(r) = r^2 \log(r)$. In TPS RBF interpolation on N scattered nodes, the approximation of a function $u(\mathbf{x})$ can be expressed as follows

$$u(\mathbf{x}) \approx \sum_{j=1}^{N} \alpha_j \phi(\|\mathbf{x} - \mathbf{x}_j\|) + \sum_{j=1}^{d+1} \alpha_{N+j} \mathcal{P}_j(\mathbf{x}), \tag{1}$$

where $\sum_{j=1}^{N} \alpha_j \mathcal{P}_{N_j}(\mathbf{x}_j) = 0$, $N_j = 1, \ldots, d+1$, and $\{\mathcal{P}_j(\mathbf{x})\}_{j=1}^{d+1}$ are the monomial basis functions in d-dimensions of total degree ≤ 1. The concept of RBF interpolation can also be implemented for solving elliptic PDE problems. We assume the solution in the form of Eq. (1). Then the coefficients α_j are determined by enforcing the PDE and boundary conditions. Let us consider the following equation

$$\mathcal{L}u(\mathbf{x}) = f(\mathbf{x}), \quad \mathbf{x} \in \Omega, \tag{2}$$

where $\mathcal{L}$ is differential operator. f is known function and the function u is unknown. The boundary condition is

$$\mathcal{B}u(\mathbf{x}) = g(\mathbf{x}), \quad \mathbf{x} \in \partial\Omega, \tag{3}$$

where $\mathcal{B}$ is linear boundary operator, g is known function and Ω is a region in $\mathbb{R}^d$. Consider $X = \{\mathbf{x}_1, \mathbf{x}_2, \ldots, \mathbf{x}_N\}$ as radial basis functions centers and $N = N_I + N_B$ where $\mathbf{x}_1, \mathbf{x}_2, \ldots, \mathbf{x}_{N_I} \in \Omega$, $\mathbf{x}_{N_I+1}, \mathbf{x}_{N_I+2}, \ldots, \mathbf{x}_N \in \partial\Omega$.

Now, by (1) into Eqs. (2) and (3), we have

$$\sum_{j=1}^{N} \alpha_j \mathcal{L}\phi(\|\mathbf{x}-\mathbf{x}_j\|) + \sum_{j=1}^{d+1} \alpha_{N+j} \mathcal{L}\mathcal{P}_j(\mathbf{x}) = f(\mathbf{x}), \quad \mathbf{x} \in \Omega, \tag{4}$$

$$\sum_{j=1}^{N} \alpha_j \mathcal{B}\phi(\|\mathbf{x}-\mathbf{x}_j\|) + \sum_{j=1}^{d+1} \alpha_{N+j} \mathcal{B}\mathcal{P}_j(\mathbf{x}) = g(\mathbf{x}), \quad \mathbf{x} \in \partial\Omega. \tag{5}$$

The collocation method is used by applying Eq. (4) at every point N_I and Eq. (5) at every point N_B as follows:

$$\sum_{j=1}^{N} \alpha_j \mathcal{L}\phi(\|\mathbf{x}_i-\mathbf{x}_j\|) + \sum_{j=1}^{d+1} \alpha_{N+j} \mathcal{L}\mathcal{P}_j(\mathbf{x}_i) = f(\mathbf{x}_i), \quad 1 \leqslant i \leqslant N_I,$$

$$\sum_{j=1}^{N} \alpha_j \mathcal{B}\phi(\|\mathbf{x}_i-\mathbf{x}_j\|) + \sum_{j=1}^{d+1} \alpha_{N+j} \mathcal{B}\mathcal{P}_j(\mathbf{x}_i) = g(\mathbf{x}_i), \quad N_I+1 \leqslant i \leqslant N.$$

This technique leads to a linear system of algebraic equations with the unknown vector of $\alpha = [\alpha_1, \alpha_2, \ldots, \alpha_{N+d+1}]^T$. By finding the unknown vector of α, we can obtain a suitable approximation for Eq. (2).

3 Mathematical formulation

3.1 Mathematical model of biosensor in CCE scheme

In the CCE scheme, the substrate ($\hat{S}$) is enzymatically E_1 transformed into the product ($\hat{P}_1$) followed by the enzymatic E_2 conversion of first product into another product that is electrochemically converted back to the first product. This scheme is

$$\begin{aligned} \hat{S} &\xrightarrow{E_1} \hat{P}_1, \\ \hat{P}_1 &\xrightarrow{E_2} \hat{P}_2, \\ \hat{P}2 &\longrightarrow \hat{P}_1, \end{aligned}$$

which by Fick's law leads to the following system of equations [2]

$$\begin{cases} \dfrac{\partial \hat{S}}{\partial \hat{t}} = D_{\hat{S}} \dfrac{\partial^2 \hat{S}}{\partial \hat{x}^2} - \dfrac{V_{\max(1)} \hat{S}}{K_M + \hat{S}}, \\ \dfrac{\partial \hat{P}_1}{\partial \hat{t}} = D_{\hat{P}_1} \dfrac{\partial^2 \hat{P}_1}{\partial \hat{x}^2} + \dfrac{V_{\max(1)} \hat{S}}{K_M + \hat{S}} - \dfrac{V_{\max(2)} \hat{P}_1}{K_M + \hat{P}_1}, \\ \dfrac{\partial \hat{P}_2}{\partial \hat{t}} = D_{\hat{P}_2} \dfrac{\partial^2 \hat{P}_2}{\partial \hat{x}^2} + \dfrac{V_{\max(2)} \hat{P}_1}{K_M + \hat{P}_1}, \quad \hat{x} \in (0, d), \quad \hat{t} > 0, \end{cases} \tag{6}$$

where $D_{\hat{S}}$ and $D_{\hat{P}_i}$ $(i = 1, 2)$ are the diffusion coefficients. $V_{\max(i)}$ and K_M are the maximal enzymatic rate and the Michaelis constant, respectively. Let $\hat{x} = 0$ represent the electrode surface and $\hat{x} = d$ is interface of the bulk solution and the enzyme membrane. The initial conditions are defined as follows:

$$\begin{cases} \hat{S}(\hat{x}, 0) = 0, & \hat{x} \in [0, d), \\ \hat{S}(d, 0) = \hat{S}_0, & \\ \hat{P}_i(\hat{x}, 0) = 0, & \hat{x} \in [0, d], \quad i = 1, 2. \end{cases} \tag{7}$$

The substrate is electro-inactive substance at the electrode surface

$$\frac{\partial \hat{S}}{\partial \hat{x}}(0, \hat{t}) = 0, \quad \hat{t} > 0. \tag{8}$$

The electrode potential is chosen to keep zero concentration of the product $\hat{P}_2$ at the electrode surface

$$\hat{P}_2(0, \hat{t}) = 0, \quad \hat{t} > 0. \tag{9}$$

Due to the electrochemical reaction, the generation rate of the product $\hat{P}_2$ at the electrode surface is proportional to the generation rate of the product $\hat{P}_1$, so we have

$$-D_{\hat{P}_2} \frac{\partial \hat{P}_2}{\partial \hat{x}}(0, \hat{t}) = D_{\hat{P}_1} \frac{\partial \hat{P}_1}{\partial \hat{x}}(0, \hat{t}), \quad \hat{t} > 0. \tag{10}$$

Assume the diffusion layer remains at a constant thickness, the concentrations of the substrate and of both products over the enzyme surface remain constant, then we have

$$\begin{cases} \hat{S}(d, \hat{t}) = \hat{S}_0, \\ \hat{P}_1(d, \hat{t}) = 0, \\ \hat{P}_2(d, \hat{t}) = 0. \end{cases} \tag{11}$$

The biosensor current depends upon the flux of the product $\hat{P}_2$ at the electrode surface. From Fick and Faraday law we have [2]:

$$\hat{i}_{CCE}(\hat{t}) = n_e F D_{\hat{P}_2} \frac{\partial \hat{P}_2}{\partial \hat{x}}(0, \hat{t}). \tag{12}$$

In order to simulation of this scheme, Eqs. (6)- (11), can be written in dimensionless form as follows:

$$\begin{cases} \dfrac{\partial S}{\partial t} = \dfrac{\partial^2 S}{\partial x^2} - \dfrac{\mu_1 S}{K+S}, \\ \dfrac{\partial P_1}{\partial t} = r_1 \dfrac{\partial^2 P_1}{\partial x^2} + \dfrac{\mu_1 S}{K+S} - \dfrac{\mu_2 P_1}{K+P_1}, \\ \dfrac{\partial P_2}{\partial t} = r_2 \dfrac{\partial^2 P_2}{\partial x^2} + \dfrac{\mu_2 P_1}{K+P_1} \end{cases} \tag{13}$$

with the initial conditions

$$\begin{cases} S(x,0) = 0, \quad x \in [0,1), \\ S(1,0) = 1, \\ P_i(x,0) = 0, \quad x \in [0,1], \quad i = 1,2, \end{cases} \tag{14}$$

and the boundary conditions

$$\begin{cases} \frac{\partial S}{\partial x}(0,t) = 0, \\ r_1 \frac{\partial P_1}{\partial x}(0,t) = -r_2 \frac{\partial P_2}{\partial x}(0,t), \\ P_2(0,t) = 0, \\ S(1,t) = 1, \quad P_i(1,t) = 0, \quad t \in [0,T], \quad i = 1,2, \end{cases} \tag{15}$$

where the normalized parameters are as follows

$$S = \frac{\hat{S}}{\hat{S}_0},\ P_i = \frac{\hat{P}_i}{\hat{S}_0},\ x = \frac{\hat{x}}{d},\ t = \frac{D_{\hat{S}}\hat{t}}{d^2},\ r_i = \frac{D_{\hat{P}_i}}{D_{\hat{S}}},\ \mu_i = \frac{V_{\max(i)} d^2}{D_{\hat{S}} \hat{S}_0},\ K = \frac{K_M}{\hat{S}_0}. \tag{16}$$

We can also write Eq. (12) as follows:

$$i_{CCE}(t) = \frac{\partial P_2}{\partial x}(0,t). \tag{17}$$

To solve Eqs. (13)- (17), we discrete the time variable using the semi-implicit backward Euler method at first. So we divide $[0,T]$ into a finite number of intervals $[t_n, t_{n+1}]$ with length Δt. Thus, in each time step we have

$$\begin{aligned} \frac{S^{n+1} - S^n}{\Delta t} &= \frac{\partial^2 S^{n+1}}{\partial x^2} - \frac{\mu_1 S^{n+1}}{K+S^n}, \\ \frac{P_1^{n+1} - P_1^n}{\Delta t} &= r_1 \frac{\partial^2 P_1^{n+1}}{\partial x^2} + \frac{\mu_1 S^{n+1}}{K+S^n} - \frac{\mu_2 P_1^{n+1}}{K+P_1^n}, \\ \frac{P_2^{n+1} - P_2^n}{\Delta t} &= r_2 \frac{\partial^2 P_2^{n+1}}{\partial x^2} + \frac{\mu_2 P_1^{n+1}}{K+P_1^n}, \end{aligned} \tag{18}$$

where $S^n := S_h(x,t_n), P_i^n := P_{ih}(x,t_n)(i=1,2)$ are known values and $S^{n+1} := S_h(x,t_{n+1}), P_i^{n+1} := P_{ih}(x,t_{n+1})(i=1,2)$ are unknown values. Now considering

$$\begin{aligned} S_h(x,t) &= \sum_{j=1}^{N} \lambda_j(t)\phi(\|x-x_j\|) + \lambda_{N+1}x + \lambda_{N+2}, \\ P_{1h}(x,t) &= \sum_{j=1}^{N} \alpha_j(t)\phi(\|x-x_j\|) + \alpha_{N+1}x + \alpha_{N+2} \\ P_{2h}(x,t) &= \sum_{j=1}^{N} \beta_j(t)\phi(\|x-x_j\|) + \beta_{N+1}x + \beta_{N+2}, \end{aligned}$$

the system (18) can be written as follows:

$$\begin{cases} \sum_{j=1}^{N}[-\Delta t\phi_{xx}(\|x_i-x_j\|) + (1+\frac{\mu_1\Delta t}{K+S_h(x_i,t_n)})\phi(\|x_i-x_j\|)]\lambda_j^{n+1} \\ \quad + (1+\frac{\mu_1\Delta t}{K+S_h(x_i,t_n)})(\lambda_{N+1}^{n+1}x_i + \lambda_{N+2}^{n+1}) = S_h(x_i,t_n), \quad i=2,\ldots,N-1, \\ \sum_{j=1}^{N}[-r_1\Delta t\phi_{xx}(\|x_i-x_j\|) + (1+\frac{\mu_2\Delta t}{K+P_{1h}(x_i,t_n)})\phi(\|x_i-x_j\|)]{\alpha_j}^{n+1} \\ \quad + (1+\frac{\mu_2\Delta t}{K+P_{1h}(x_i,t_n)})(\alpha_{N+1}^{n+1}x_i + \alpha_{N+2}^{n+1}) \\ \quad - \frac{\mu_1\Delta t}{K+S_h(x_i,t_n)}(\sum_{j=1}^{N}\phi(\|x_i-x_j\|)\lambda_j^{n+1} + \lambda_{N+1}^{n+1}x_i + \lambda_{N+2}^{n+1}) \\ \quad = P_{1h}(x_i,t_n), \quad i=2,\ldots,N-1, \\ \sum_{j=1}^{N}[-r_2\Delta t\phi_{xx}(\|x_i-x_j\|) + \phi(\|x_i-x_j\|)]\beta_j^{n+1} + \beta_{N+1}^{n+1}x_i + \beta_{N+2}^{n+1} \\ \quad - \frac{\mu_2\Delta t}{K+P_{1h}(x_i,t_n)}(\sum_{j=1}^{N}\alpha_j^{n+1}\phi(\|x_i-x_j\|) + \alpha_{N+1}^{n+1}x_i + \alpha_{N+2}^{n+1}) \\ \quad = P_{2h}(x_i,t_n), \quad i=2,\ldots,N-1. \end{cases} \tag{19}$$

By applying boundry conditions (15) in $x_1,\ x_N$ and considering conditions

$$\begin{aligned} \sum_{j=1}^{N}\lambda_j^{n+1} &= \sum_{j=1}^{N}\lambda_j^{n+1}x_j = \sum_{j=1}^{N}\alpha_j^{n+1} = \sum_{j=1}^{N}\alpha_j^{n+1}x_j \\ &= \sum_{j=1}^{N}\beta_j^{n+1} = \sum_{j=1}^{N}\beta_j^{n+1}x_j = 0, \end{aligned}$$

we obtain a linear algebraic system with the unknown vector $[\lambda_1^{n+1}, \lambda_2^{n+1}, \ldots, \lambda_{N+2}^{n+1}, \alpha_1^{n+1}, \alpha_2^{n+1}, \ldots, \alpha_{N+2}^{n+1}, \beta_1^{n+1}, \beta_2^{n+1}, \ldots, \beta_{N+2}^{n+1}]^T$.

3.2 Mathematical model of biosensor in CEC scheme

In this scheme, the substrate is enzymatically converted to the product $\hat{P}_1$ followed by the electrochemical conversion of the product $\hat{P}_1$ to another product $\hat{P}_2$ that in turn is enzymatically converted back to $\hat{P}_1$ as follows

$$\begin{aligned} \hat{S} &\xrightarrow{E_1} \hat{P}_1, \\ \hat{P}_1 &\longrightarrow \hat{P}_2, \\ \hat{P}_2 &\xrightarrow{E_2} \hat{P}_1. \end{aligned}$$

With the Fick's law, we have [2]

$$\begin{cases} \dfrac{\partial \hat{S}}{\partial \hat{t}} = D_{\hat{S}} \dfrac{\partial^2 \hat{S}}{\partial \hat{x}^2} - \dfrac{V_{\max(1)} \hat{S}}{K_M + \hat{S}}, \\ \dfrac{\partial \hat{P}_1}{\partial \hat{t}} = D_{\hat{P}_1} \dfrac{\partial^2 \hat{P}_1}{\partial \hat{x}^2} + \dfrac{V_{\max(1)} \hat{S}}{K_M + \hat{S}} + \dfrac{V_{\max(2)} \hat{P}_2}{K_M + \hat{P}_2}, \\ \dfrac{\partial \hat{P}_2}{\partial \hat{t}} = D_{\hat{P}_2} \dfrac{\partial^2 \hat{P}_2}{\partial \hat{x}^2} - \dfrac{V_{\max(2)} \hat{P}_2}{K_M + \hat{P}_2}, \quad \hat{x} \in (0, d), \quad \hat{t} > 0. \end{cases} \tag{20}$$

The notations are the same as in the model of a biosensor acting in the CCE scheme. The initial conditions are the same as in the case of CCE scheme. When the biosensor acts in the CEC mode, the electrode potential is chosen to keep zero concentration of the product $\hat{P}_1$ at the electrode surface, i.e.,

$$\hat{P}_1(0, \hat{t}) = 0, \quad \hat{t} > 0. \tag{21}$$

The dimensionless equations are as follows:

$$\begin{cases} \dfrac{\partial S}{\partial t} = \dfrac{\partial^2 S}{\partial x^2} - \dfrac{\mu_1 S}{K + S}, \\ \dfrac{\partial P_1}{\partial t} = r_1 \dfrac{\partial^2 P_1}{\partial x^2} + \dfrac{\mu_1 S}{K + S} + \dfrac{\mu_2 P_2}{K + P_2}, \\ \dfrac{\partial P_2}{\partial t} = r_2 \dfrac{\partial^2 P_2}{\partial x^2} - \dfrac{\mu_2 P_2}{K + P_2}, \end{cases} \tag{22}$$

with the initial conditions

$$\begin{cases} S(x, 0) = 0, \quad x \in [0, 1), \\ S(1, 0) = 1, \\ P_i(x, 0) = 0, \quad x \in [0, 1], \quad i = 1, 2, \end{cases} \tag{23}$$

and the boundry conditions

$$\begin{cases} \frac{\partial S}{\partial x}(0,t)=0, \\ -r_1\frac{\partial P_1}{\partial x}(0,t)=r_2\frac{\partial P_2}{\partial x}(0,t), \\ P_1(0,t)=0, \\ S(1,t)=1, \quad P_i(1,t)=0, \quad t\in[0,T]. \end{cases} \tag{24}$$

The biosensor current depends upon the flux of the product P_1 at the electrode surface:

$$i_{CEC}(t)=\frac{\partial P_1}{\partial x}(0,t). \tag{25}$$

To solve Eqs. (22)-(25), in the CEC mode, the governing equations can be approximated similarly as in the case of the CCE mode. Then (22) can be discretized as follows:

$$\begin{cases} \sum_{j=1}^{N}[-\Delta t\phi_{xx}(\|x_i-x_j\|)+(1+\frac{\mu_1\Delta t}{K+S_h(x_i,t_n)})\phi(\|x_i-x_j\|)]\lambda_j^{n+1} \\ \quad +(1+\frac{\mu_1\Delta t}{K+S_h(x_i,t_n)})(\lambda_{N+1}^{n+1}x_i+\lambda_{N+2}^{n+1})=S_h(x_i,t_n), \quad i=2,\ldots,N-1, \\ \sum_{j=1}^{N}[-r_1\Delta t\phi_{xx}(\|x_i-x_j\|)+\phi(\|x_i-x_j\|)]{\alpha_j}^{n+1}+\alpha_{N+1}^{n+1}x_i+\alpha_{N+2}^{n+1} \\ \quad -\frac{\mu_1\Delta t}{K+S_h(x_i,t_n)}(\sum_{j=1}^{N}\phi(\|x_i-x_j\|)\lambda_j^{n+1}+\lambda_{N+1}^{n+1}x_i+\lambda_{N+2}^{n+1}) \\ \quad -\frac{\mu_2\Delta t}{K+P_{2h}(x_i,t_n)}(\sum_{j=1}^{N}\phi(\|x_i-x_j\|)\beta_j^{n+1}+\beta_{N+1}^{n+1}x_i+\beta_{N+2}^{n+1}) \\ \quad =P_{1h}(x_i,t_n), \quad i=2,\ldots,N-1, \\ \sum_{j=1}^{N}[-r_2\Delta t\phi_{xx}(\|x_i-x_j\|)+(1+\frac{\mu_2\Delta t}{K+P_{2h}(x_i,t_n)})\phi(r_{ij})]\beta_j^{n+1} \\ \quad +(1+\frac{\mu_2\Delta t}{K+P_{2h}(x_i,t_n)})(\beta_{N+1}^{n+1}x_i+\beta_{N+2}^{n+1})=P_{2h}(x_i,t_n), \quad i=2,\ldots,N-1. \end{cases} \tag{26}$$

By applying boundry conditions (15) in $x_1,\ x_N$ and considering conditions

$$\begin{aligned} \sum_{j=1}^{N}\lambda_j^{n+1} &= \sum_{j=1}^{N}\lambda_j^{n+1}x_j=\sum_{j=1}^{N}\alpha_j^{n+1}=\sum_{j=1}^{N}\alpha_j^{n+1}x_j \\ &= \sum_{j=1}^{N}\beta_j^{n+1}=\sum_{j=1}^{N}\beta_j^{n+1}x_j=0, \end{aligned}$$

we get a linear algebraic system with the unknown vector $[\lambda_1^{n+1},\lambda_2^{n+1},\ldots,\lambda_{N+2}^{n+1},\alpha_1^{n+1},\alpha_2^{n+1},\ldots,\alpha_{N+2}^{n+1},\beta_1^{n+1},\beta_2^{n+1}\ldots,\beta_{N+2}^{n+1}]^T$.

4 Numerical Simulation

In this section, we will report the numerical simulation of biosensors including two schemes CCE and CEC. Our numerical experiments are carried out in MATLAB software. For calculations, $N = 201$, $\Delta t = 0.05$, $d = 100\mu m$, $D_{\hat{s}} = D_{\hat{P}_1} = D_{\hat{P}_2} = 300\mu m^2/s$, $K_M = 100\mu M$ and $\hat{S}_0 = 100\mu M$ are chosen. In Figures 1 and 2, the profiles of the substrate concentration as well as the products concentration in the enzyme layer are presented for biosensors acting in CCE and CEC modes.

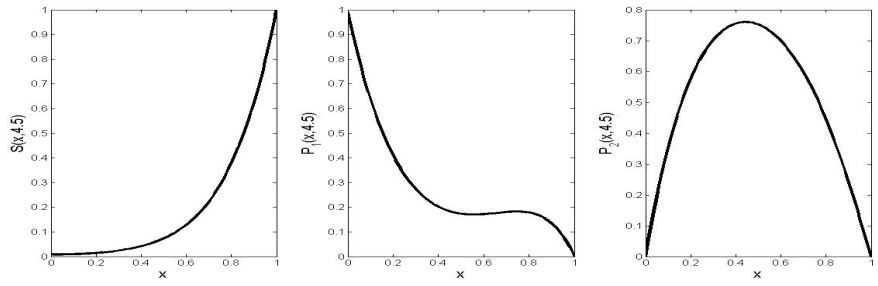

Figure 1: The profile of the substrate and the products concentration in enzyme layer acting in CCE mode.

In these figures, we consider the maximal enzymatic rate $V_{\max(1)} = V_{\max(2)} = 100\mu M/s$. For both biosensors, the concentration of the substrate at steady-state condition is approximately the same. In both figures, the results are similar to those obtained in [1, 2].

At the steady state, $t \longrightarrow \infty$, $S(x,t) + P_1(x,t) + P_2(x,t) = 1$ is valid for all $x \in [0,1]$ [2]. In order to efficient performance of the proposed method, since there is not exact solution for the study models, the absolute residual error function is given as $\delta(T) = |S(x,T) + P_1(x,T) + P_2(x,T) - 1|$ in both CCE and CEC modes. Figures 3 and 4 report the graph of the absolute residual error function in CCE and CEC modes, respectively.

4.1 The effect of response amplification

One of the most important characteristics of the trigger is response amplification [2]. The steady-state current is similar for both type of biosensors, $i_{CCE}(4.5) \approx 4.22$, $i_{CEC}(4.5) \approx 4.41$. The time of steady-state is also approximately the same in both modes. In Figure 5, we can observe the steady-state current with and without amplification. This figure shows the steady-state current is amplified in triggering mode. In order to compare

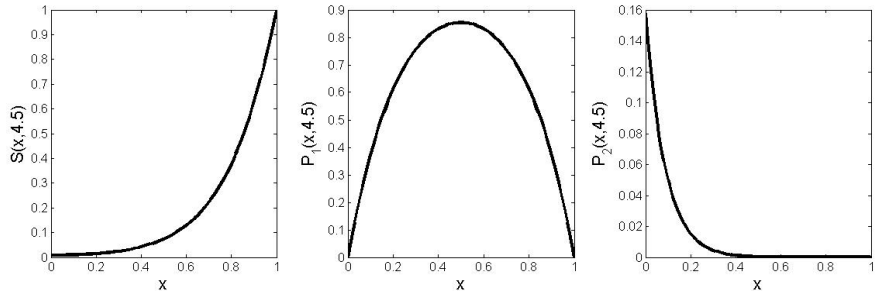

Figure 2: The profile of the substrate and the products concentration in enzyme layer acting in CEC mode.

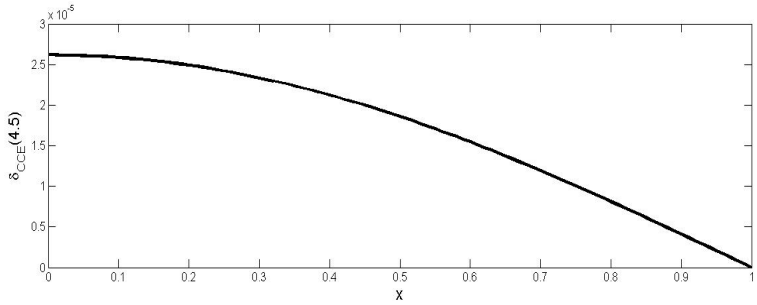

Figure 3: The graph of the absolute residual error function in CCE mode.

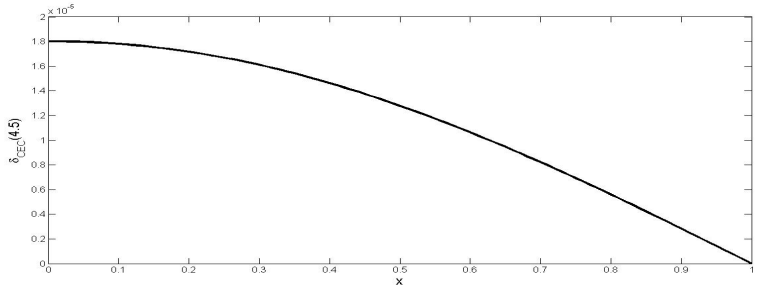

Figure 4: The graph of the absolute residual error function in CEC mode.

the biosensor response with and without amplification, the gain of the sensitivity is defined as the ratio of the steady-state current of the trigger biosensor to the steady-state current of biosensor without amplification as follows

$$\begin{cases} G_{CCE} = \frac{i_{CCE}}{i}, \\ G_{CEC} = \frac{i_{CEC}}{i}. \end{cases} \tag{27}$$

By using the calculation of G_{CCE} and G_{CEC}, we can see the steady-state current increases up to about 10 times in both schemes.

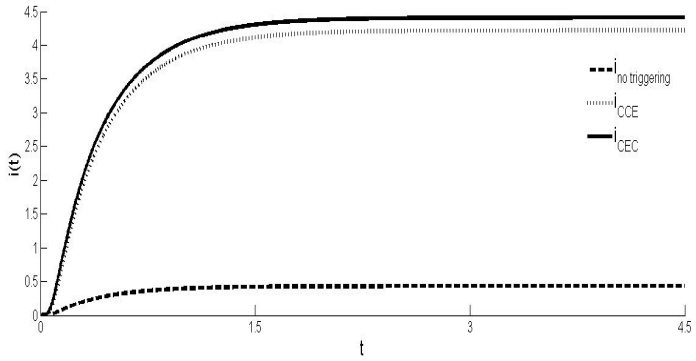

Figure 5: The current profile with and without amplification.

4.2 The influence of the normalized Michaelis constant on the gain of sensitivity.

The most differences in gain of the sensitivity is in high substrate concentrations i.e. ($\hat{S}_0 > K_M$). Table 1 shows the steady-state current density for the various normalized Michaelis constants ($K = 0.1, 1, 10$) with $\hat{S}_0 = 100\mu M$. We can see the higher steady-state current in $K = 0.1$. In the normalized Michaelis constant $K = 0.1$, the substrate concentration is 10 times higher than Michaelis constant.

Table 1: the steady state current for different normalized Michaeelis constants.

K	0.1	1	10
i_{CCE}	$6.97E0$	4.22E0	$7.4E-1$
i_{CEC}	$6.96E0$	4.41E0	$1.26E0$

4.3 The influence of maximal enzymatic rates on steady-state current.

As Tables 2 and 3 show, the steady-state current is monotonously increasing functions of both arguments $V_{\max(1)}$ and $V_{\max(2)}$ in CCE and CEC modes. In these calculations, $V_{\max(1)}$ and $V_{\max(2)}$ varied from $1\mu M/s$ to $1000\mu M/s$.

Table 2: The steady-state current density in $V_{\max(2)} = 1000\mu M/s$ for different $V_{\max(1)}$.

$V_{\max(1)}$	1	10	100	1000
i_{CCE}	1.16E-1	$1.21E0$	$8.16E0$	$1.34E+1$
i_{CEC}	1.37E-1	$1.30E0$	$8.23E0$	$1.34E+1$

Table 3: The steady-state current density in $V_{\max(1)} = 1000\mu M/s$ for different $V_{\max(2)}$.

$V_{\max(2)}$	1	10	100	1000
i_{CCE}	$8.16E-2$	$7.64E-1$	$4.35E0$	$1.34E+1$
i_{CEC}	$1.06E0$	$1.57E0$	$4.44E0$	$1.34E+1$

Table 3 shows that the variations of $V_{\max(2)}$ has weak effect on current density in CEC because of high substrate concentration. When $V_{\max(2)} > 0$, the enzyme E_2 is active. In CCE mode, the active enzyme E_2 has a critical role in biosensor current. We can observe from Table 4 in the case of $V_{\max(2)} = 0$ even if the activity of an enzyme E_1 is very high, the biosensor current would be zero. However, in CEC mode, when $V_{\max(2)} = 0$ the biosensor still generate the current if $V_{\max(1)} > 0$. In this case, the biosensor response in CEC mode is the same as biosensor response without an amplification.To investigate this, the steady-state current of no-triggering biosensor has been calculated at the same condition as above.

Table 4: The steady-state current in CEC mode in the case of $V_{\max(2)} = 0$.

$V_{\max(1)}$	1	10	100	1000
i_{CCE}	0	0	0	0
i_{CEC}	$7.97E-2$	$5.63E-1$	$9.91E-1$	$1.02E0$
$i_{no-triggering}$	$7.97E-2$	$5.63E-1$	$9.91E-1$	$1.02E0$

4.4 The influence of substrate concentration on steady state current

As Table 5 shows, the behavior of the biosensor response versus the substrate concentration is very similar in both schemes. The most differences is in high substrate concentration.

Table 5: The steady state current density for different substrate concentrations.

$\hat{S}_0$	0.1	10	1000
i_{CCE}	$5.46E-3$	$5.30E-1$	$1.38E+1$
i_{CEC}	$5.57E-3$	$5.41E-1$	$2.16E+1$

5 Conclusions

In this paper, we studied the numerical simulation of biosensors including two schemes CCE and CEC. The meshfree collocation method based on TPS radial basis function in space variable and the semi-implicit backward Euler in time variable were proposed to simulate mathematical modeling of biosensors. In this study, the behaviour of biosensors versus various parameters such as normalized Michaelis constant, maximal enzymatic rates and substrate concentration were carried out. In order to compare the response of biosensor with and without amplification, the gain of the sensitivity was studied. In this study, we observed that steady-state current increased up in both scheme. The most differences in gain of the sensitivity was in high substrate concentration. We concluded that the gain of sensitivity decreased with increase in substrate consentration. As maximal enzymatic rates $V_{\max(1)}$, $V_{\max(2)}$ have a noticeable role in biosensor response, we checked them in our simulations. We achieved that the steady-state current of a triggering biosensor is monotonously increasing functions of both maximal enzymatic rates. Since in CCE mode, the active enzyme E_2 has a critical role in biosensor current, the biosensor response would be zero at $V_{\max(2)} = 0$. We showed that in CEC mode if $V_{\max(2)} = 0$, the biosensor response in CEC mode is the same as biosensor response without an amplification. We also investigated that the most differences in the biosensor response is in high substrate concentration.

Acknowledgment

The authors are grateful to three reviewers for their constructive comments on the manuscript.

References

[1] R. Baronas, J. Kulys and F. Ivanauskas, *Mathematical model of the biosensors acting in a trigger mode*, Sensors **4** (2004) 20-36.

[2] R. Baronas, J. Kulys and F. Ivanauskas, *Mathematical modeling of biosensors: an introduction for chemists and mathematicians*, Springer, 2010.

[3] R. Baronas, F. Ivanauskas, J. kulys and M. Sapagovas, *Computational modeling of a sensor based on an array of enzyme microreactors*, Nonlinear Anal. Model. Contr. **9** (2004) 203-218.

[4] W. Chen, Z.J. Fu and C.S. Chen, *Recent advances in radial basis function collocation methods*, Springer, 2014.

[5] G. Demirkaya, C. Wafo Soh and O.J. Ilegbusi, *Direct solution of Navier-Stokes equations by radial basis functions*, Appl. Math. Model. **32** (2008) 1848-1858.

[6] A. Eswari and L. Rajendran, *Analyical solution of steady state current at a microdisk biosensor*, J. Electronal. Chem. **641** (2010) 35-44.

[7] G.E. Fasshauer, *Meshfree approximation methods with* MATLAB, World Scientific, 2007.

[8] B. Fuhrmann and U. Spohn, *An enzymatic amplification flow injection analysis (FIA) system for the sensetive determination of phenol*, Biosens. Bioelectron. **13** (1998) 895-902.

[9] J. Kulys, *The development of new analytical systems based on biocatalysts*, Anal. Lett. **14** (1981) 377-397.

[10] J. Lin, S. Reutskiy, C. S. Chen and J. Lu, A novel method for solving time dependent 2D advection diffusion reaction equations to model transfer in nonlinear anisotropic media, Commun. Comput. Phys. **26** (2019) 233-264.

[11] S. Ling-De, J. Zi-Wu and J.Tong-Song, *Numerical method based on radial basis functions for solving reaction-diffusion equations*, IEEE Information Tech, Networking, Electro and Automation Control Conference, IEEE, 2016.

[12] S. Loghambal and L. Rajendran, *Mathematical modeling of diffusion and kinetics in amperometric Immobilical enzyme electrodes*, Electrochem. Acta, **55** (2010) 5230-5238.

[13] H. R. Luckarift, *Silica-immobilized enzyme reactors*, J. Liq. Chromatogr. R.T. **31** (2008) 1568-1592.

[14] N. Milozic, M. Lubej, M. Lakner, P. Znidarsic-Plazl and I. Plazl. *Theoretical and experimental study of enzyme kinetics in a microreactor system with surface-immobilized biocatalyst*, Chem. Eng. J. **313** (2017) 374-381.

[15] M. Mohammadi, R. Mokhtari and R. Schaback, *Meshless method for solving the 2D Brusselator reaction-diffusion system*, CMES. **101** (2014) 113-138.

[16] R. Popovtzer, T. Neufeld and E. Z. Ron, *Electrochemical detection of biological reactions using a novel nano-bio-chip array*, Sensor Act. B-Chem. **119** (2006) 664-672.

[17] A. N. Reshetilov and A. M. Bezborodov, *Nanobiotechnology and biosensor research*, Appl. Biochem. Micro. **44** (2008) 1-5.

[18] E. Shivanian and H. Fatahi, *Analysis of meshless local radial point interpolant on a model in population dynamics*, Comput. Methods Differ. Equ. **7**(2019) 276-288.

[19] E. Shivanian and A. Jafarabadi, *Turing models in the biological pattern formation through spectral meshless radial point interpolation approach*, Eng. Comput. **36** (2020) 271-282.

[20] T. Skybov, M. Pribyl and P. Hasal, *Mathematical model of decolourization in a rotating disc reactor*, Biochem. Eng. J. **93** (2015) 151-165.

[21] A. P. F. Turner, I. Karube and G. S. Wilson, *Biosensors: fundamentals and applications*, Oxford U.P, 1987.

[22] P. L. Urban, D. M.Goodall and N. C.Bruce, *Enzymatic microreactors in chemical analysis and kinetic studies*, Biotechnol. Adv. **24** (2006) 42-57.

[23] V. Vojinovic, F. M. F. Esteves, J. M. S. Cabral and L.P. Fonseca, *Bienzymatic analytical microreactors for glucose, lactate, ethanol, galatose and l-amino acid monitoring in cell culture media*, Anal. Chim. Acta, **565** (2006) 240-249.

[24] U. Wollenberger, F. Schubert, D. Pfeiffer and F.W. Scheller, *Enhancing biosensor performance using multienzyme systems*, Trends. Biotechnol. **11** (1993) 255-262.